STRENGTH AND DUCTILITY OF RETROFITTED R/C BUILDING BY MULTI-STORY STEEL-BRACED FRAME SUBJECTED TO TRI-LATERAL EARTHQUAKE LOADING

KITAYAMA Kazuhiro[1] and NAKANUMA Hiroki[2]

[1] *Associate Professor, Dept. of Architecture, Tokyo Metropolitan University, Tokyo, Japan*
[2] *Engineer, Takenaka Corporation, Osaka, Japan*
Email: kitak@tmu.ac.jp

ABSTRACT :

Lateral resistance and deformation capacity of a retrofitted reinforced concrete building by a multi-story steel-braced frame were studied by a tri-lateral static loading test using a plane frame specimen with 2-stories and 3-bays. R/C columns close to the steel-braced frame failed in tension, resulted from the tensile yielding and the fracture of all longitudinal bars. The lateral shear capacity and the deformation capacity were degraded under tri-lateral loading by severe compressive damage of concrete at the bottom of the columns due to bi-axial bending compared with those under in-plane and axial loading.

KEYWORDS: reinforced concrete, retrofit, steel-brace, strength, ductility, tri-lateral loading

1. INTRODUCTION AND OBJECTIVE

For seismic retrofit of existing reinforced concrete (R/C) buildings, a steel-braced frame, which consists of a V-shaped steel brace enclosed by perimeter steel rims, is often installed into a moment resisting frame with adequate clearance. These are connected through no-shrinkage mortar injection into the clearance using stud connectors welded to steel rims and post-installed anchors embedded to R/C beams and columns. It is most desirable that the one of diagonal chords in the steel-braced frame yields in tension and the other buckles in compression under earthquake excitations. The column tension failure, however, occurs frequently prior to the preferable failure mechanism, which is caused at the bottom of a barbell-shaped cross section by tensile yielding of all longitudinal bars in a R/C boundary column adjacent to the steel-braced frame, when some steel-braced frames are placed over multi-stories in an existing R/C frame. Therefore, lateral resistance and deformation capacity under tri-lateral earthquake loads were studied by static loading test for a R/C frame retrofitted by a multi-story steel-braced frame, focusing on the column tension failure, and were compared with those obtained by the previous test conducted under the in-plane horizontal and axial loads (Kitayama, Ref. 1).

2. OUTLINE OF TEST

2.1 Specimen

Reinforcement details and section dimensions are shown in **Fig. 1**. A quarter-scale plane retrofitted R/C frame specimen (called as Specimen No.3) was tested in this study. The specimen had three bays with a span length of 1000 mm and two stories with a height of 800 mm, with a multi-story steel-braced frame in the central bay. Configuration of the specimen, member length, section dimensions of R/C beams, columns and the steel-braced frame and reinforcement arrangement were same as those for Specimen No.2 tested by the author (Ref. 1).

Specimen No.3 was designed to result in the column tension failure at the bottom of the combined cross section of barbell-shape with the steel-braced frame and boundary R/C columns denoted as Column 2 and 3 in **Fig. 1**. The amount of longitudinal bars in boundary columns was reduced compared with that in exterior columns denoted as Column 1 and 4 in **Fig.1** to cause the column tension failure. R/C beams and columns were designed according to the weak-beam strong-column concept. A column in R/C buildings designed by old seismic regulations in Japan tends to fail in shear during earthquakes. Note that, however, R/C columns in the specimen was designed to not fail in shear but develop flexural yielding at both end hinge regions because the objective

of the paper was to investigate the earthquake resistant performance for the column tension failure, and column shear failure was likely to affect significantly the seismic behavior of the specimen.

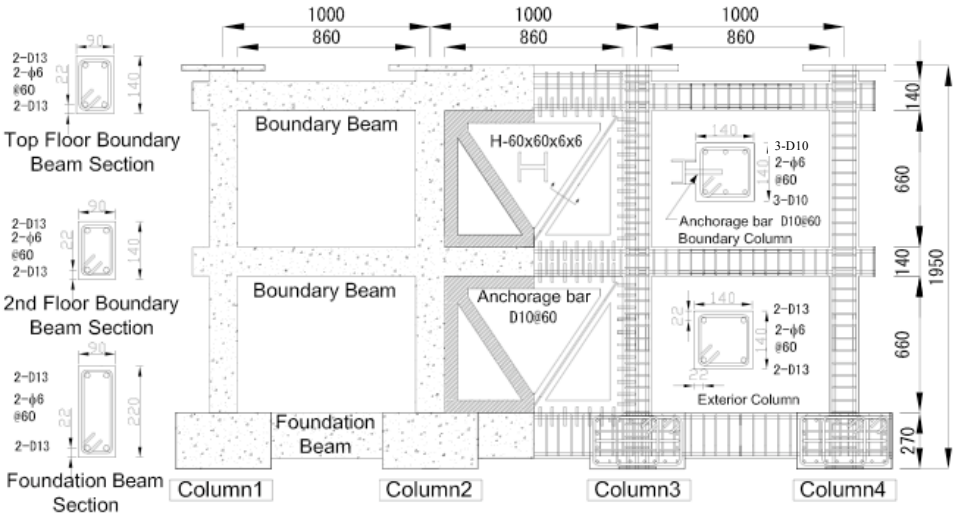

Figure 1 : Reinforcement details and section dimensions

The steel-braced frame had a H-shaped cross section of 60 mm width and 60 mm depth, which was built by welding flat plates with 6 mm thickness. Details of connection between a R/C member and a steel rim are illustrated in **Fig. 1**. Anchorage bars of D10 were welded in a row to perimeter steel rims with a spacing of 60 mm and an embedment length of 63 mm from the extreme fiber of a R/C cross section of beams and columns. Although non-shrinkage mortar is injected into the gap between the steel-braced frame and existing R/C members to connect fast each other for actual practice, mortar injection was omitted in construction of the specimen for the simplicity of fabrication, and concrete was cast in the horizontal position with the steel-braced frame in place, which was set already at proper position into reinforcement cages of beams and columns. Note that this connecting method intensifies the unification between the steel-braced frame and R/C members, and seems to hardly affect the pull-out of anchorage bars compared with that in practice using drilling and grouting. Material properties of concrete and steel for Specimens No.3 and No.2 tested previously are listed in **Table 1**. Concrete compressive strength was 30 MPa approximately by cylinder tests.

Table 1 : Material properties

(a) Steel		Yield strength, MPa	Tensile strength, MPa	Yield strain
Column longi. bar D10 (SD295)	No.2	368	503	0.20%
	No.3	379	492	0.20%
Column longi. bar D13 (SD390)	No.2	430	602	0.24%
	No.3	456	660	0.23%
Beam longi. bar D13 (SD345)	No.2	346	470	0.19%
	No.3	377	544	0.21%
Shear reinforce. bar ϕ6	No.2	589	630	0.28%
	No.3	407	494	0.19%
Anchorage bar D10 (SD345)	No.2	383	526	0.22%
	No.3	384	547	0.21%
Steel-brace (SM490)	No.2	435	551	0.21%
	No.3	280	375	0.14%

(b) Concrete	Comp. Strength, MPa	Secant modulus, x10^4 MPa	Strain at comp. strength	Tensile strength, MPa
No.2	30.3	2.80	0.22%	2.44
No.3	37.0	3.12	0.22%	2.67

2.2 Loading Method and Instrumentation

The loading system is shown in **Fig. 2**. At first, constant axial load of 160 kN was applied to the steel-braced frame and boundary R/C columns by a vertical center jack. Axial load to two exterior columns was not applied because of the damage by an accident as mentioned later, but that equal to 40 kN was applied for Specimen No.2. Second, an out-of-plane deflection angle of 1.5 % was given by three oil jacks in the south-north direction attached at the top of the specimen to cause flexural yielding at the bottom critical section of columns. Finally, in-plane horizontal load reversals were applied to a center of the specimen by two oil jacks in the east-west direction keeping the out-of-plane deflection constant. Test result was compared with that of an accompanying plane specimen No.2 subjected to in-plane loading alone, namely without out-of-plane loading, to identify the influence of the horizontal bi-directional loading. The footings of the specimen were fixed to R/C reaction floor by PC tendons.

Specimen was controlled by a drift angle for one loading cycle of 0.25 %, two cycles of 0.5 % and 1 % respectively, one cycle of 1.5 %, two cycles of 2 % and one cycle of 3 %. The out-of-plane drift angle is defined as the horizontal displacement at the center of a top floor beam divided by the height between the top

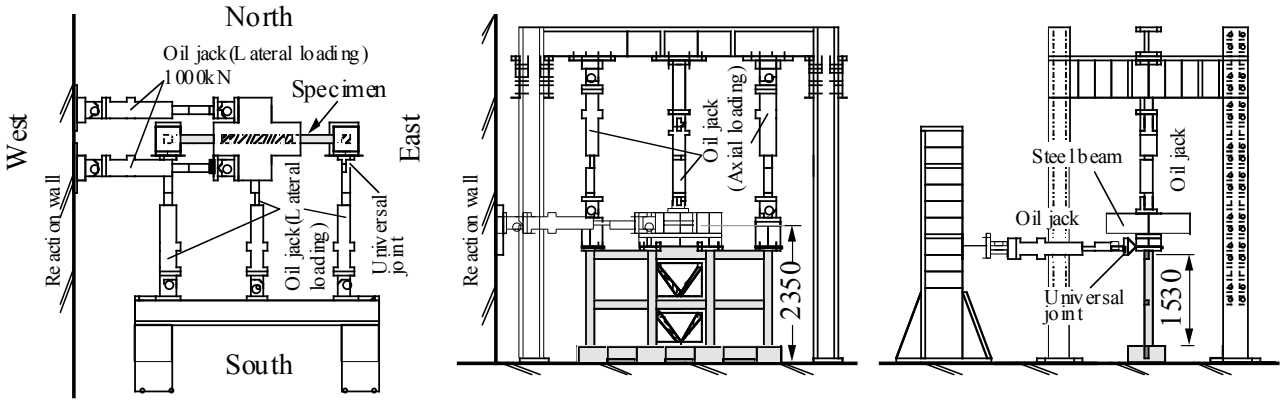

(a) Plan view (b) South elevation (c) East elevation

Figure 2 : Loading apparatus

fiber of the foundation and the center of a top floor beam, i.e., 1530 mm. The in-plane drift angle is defined as the horizontal displacement at the center of horizontal jacks in the east-west direction divided by the height between the slab top of the reaction floor and the center of the jacks, i.e., 2350 mm.

Lateral force and axial load were measured by load-cells located at the end of each oil jack. Horizontal displacements at the point of load application in the longitudinal direction and at the center of top and second floor beams, and local rotation in a plastic hinge region of beams and columns were measured by displacement transducers. Strains of beam and column longitudinal bars, vertical and diagonal steel chords of the braced frame and anchorage bars at the bottom of the first-story steel-braced frame were measured by strain gauges.

2.3 Influence of Accident on Test

Excessive axial load equal to 581 kN, corresponding to the axial stress of 0.74 times the concrete compressive strength, was applied for Specimen No.3 by an accident in jack control operation to two exterior columns, which were scheduled to bear an axial load of 40 kN respectively. This accident caused the out-of-plane buckling of Column 1 at the top of and Column 4 at the bottom of the second-story column respectively accompanied by spall-off of the shell concrete in the north surface in the buckling region, and several torsional cracks along the top boundary beams with tensile yielding of longitudinal bars at the face of Columns 2 and 3. The accident was judged, however, to affect hardly seismic behavior for the specimen after cracking, since the out-of-plane shear force was applied toward the south direction opposed to the buckling direction to result in compression in a south side, i.e., sound concrete, of the cross section of buckled columns.

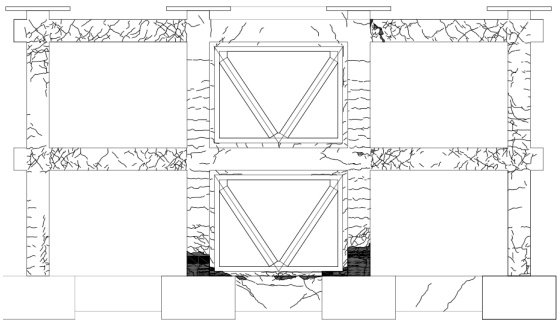

Figure 3 : Crack pattern of Specimen No.3

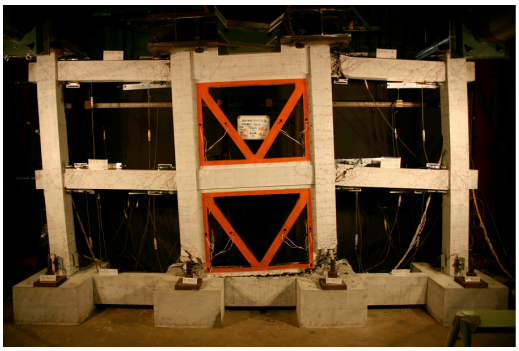

Photo. 1 : Column tension failure of Specimen No.3 under tri-lateral loading

3. TEST RESULTS

3.1 Failure Process

The column tension failure occurred for Specimen No.3. The

failure pattern at the end of the test is shown in **Fig. 3** and **Photo. 1**. Many flexural cracks and severe crushing of concrete at the bottom region were observed for boundary columns. Buckling and eventual fracture of all longitudinal bars occurred at the bottom region in boundary columns. The steel-braced frame separated widely at the base from the R/C foundation beam, resulting in the pull-out of anchorage bars between them. Diagonal shear cracks developed in boundary beams after flexural cracking.

3.2 Out-of-plane Behavior

Out-of-plane shear force – drift angle relationship is shown in **Fig. 4**. The shear force is the force given by the central jack alone, i.e., resisted by two boundary columns in the south-north direction. Solid lines represent the force – drift relations for each story, a horizontal broken line the sum of the yield strength for two boundary columns predicted briefly and vertical broken lines the yield deflections for each story computed by Sugano's formula. The predicted yield strength and deflection agreed well with test result. The out-of-plane shear force descended during in-plane loading sustaining the out-of-plane drift angle of 1.5 % due to bi-axial bending of R/C boundary columns, and was almost lost at the peak strength under in-plane loading.

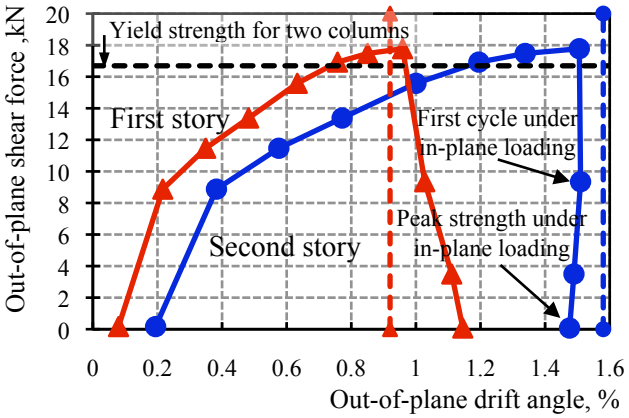

Figure 4 : Out-of-plane shear force – drift relation

3.3 In-plane Behavior

In-plane shear force – drift angle relationship is shown in **Fig. 5(a)** for Specimen No.3 and **Fig. 5(b)** for Specimen No.2 tested previously without out-of-plane loading. The in-plane shear force is defined as the horizontal force applied by two oil jacks in the east-west direction corrected for the P-Delta effect resulting from axial load.

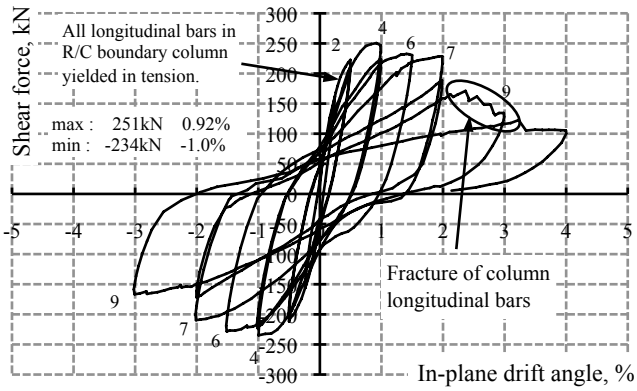

(a) Specimen No.3 under tri-lateral loading

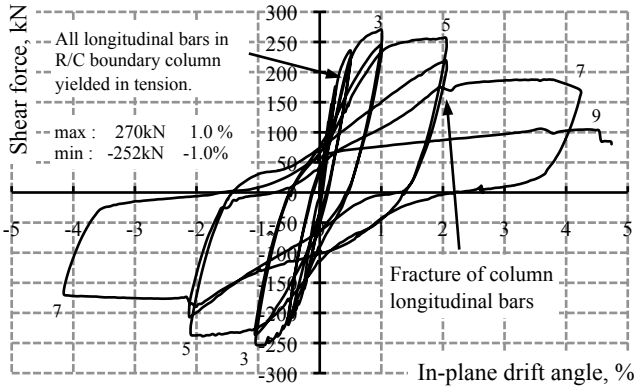

(b) Specimen No.2 without out-of-plane loading

Figure 5 : In-plane shear force – drift angle relations

As illustrated in **Fig. 5(a)**, all longitudinal bars in a R/C boundary column yielded in tension at a drift angle of 0.38 %. Bond deterioration occurred at a drift angle of 0.4 % along anchorage bars connecting the steel-braced frame and the R/C foundation beam. The lateral resistance reached the peak capacity of 251 kN at a drift angle of approximately 1 %, forming plastic hinges at the end of all boundary beams and separating between the steel-braced frame and the R/C foundation beam with an opening width of 6 mm. While the lateral resistance diminished gradually by concrete crushing, the fracture of column longitudinal bars at the bottom of both boundary columns caused remarkable degradation of the resistance after a drift angle of 2 %. Hysteresis loops showed a stable spindle shape until a drift angle of 2 %.

The peak lateral capacity with out-of-plane loading for Specimen No.3 was 0.93 times that without out-of-plane loading for Specimen No.2, for which the peak strength was 270 kN and the failure process was almost similar to that for Specimen No.3.

4. DISCUSSIONS

4.1 Lateral Resistance Carried by Diagonal Chords in Steel-Braced Frame

The lateral force carried by two diagonal steel chords in the first story steel-braced frame, which can be obtained as a horizontal component of the axial force in these chords subjected to tension and compression respectively, and was computed from measured strain at these chords, is shown in **Fig. 6** for Specimen No.3 by a thick line, with the whole lateral resistant force for the specimen by a thin line. The lateral force carried by two diagonal chords attained the peak strength at an in-plane drift angle of 0.75 %, which shared 51 percent of the whole lateral resistance, and decreased. The peak strength for diagonal steel chords was attributed to the pull-out of anchorage bars connecting the steel-braced frame and the R/C foundation beam.

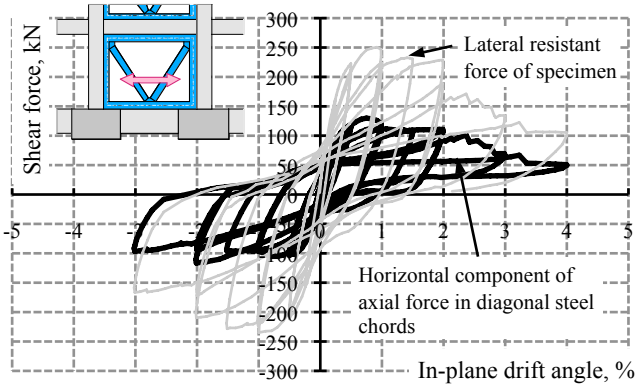

Figure 6 : Horizontal resultant force of diagonal chords in steel-braced frame

4.2 Lateral Strength

The lateral strength, Q_{max}, obtained by the test is compared with the predicted strength, Q_{cal}, by Eqn. 4.1, listed in **Table 2**.

$$Q_{cal} = Q_{Bf} + Q_{c1} + Q_{c4} \qquad (4.1)$$

where Q_{Bf} is the lateral shear resistance shared by the steel-braced frame with two R/C boundary columns which can be computed by moment equilibrium as illustrated in **Fig. 7** with the expression of Eqn. 4.2.

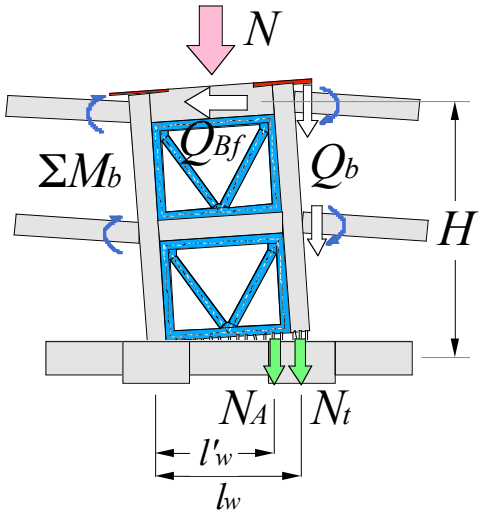

Figure 7 : Lateral shear resistance by steel-braced frame with R/C boundary columns

$$Q_{Bf} = (\Sigma M_b + l_w(\Sigma Q_b + 0.5N + N_t) + l_w' N_A) / H \qquad (4.2)$$

where ΣM_b : sum of the flexural ultimate moment of boundary beams connecting to the steel-braced frame, ΣQ_b : sum of the shear force of two boundary beams connecting to the tensile boundary column, l_w : center-to-center distance between R/C boundary columns, i.e., 1000 mm, N : compressive axial load imposed to the steel-braced frame, i.e., 160 kN, N_t : tensile force induced to the R/C boundary column in tension, i.e., a product of the total sectional area and yield strength of a longitudinal bar in the column, l_w' : distance from a center of the R/C boundary column in compression to an anchorage bar located in the extreme side in tension, i.e., 875 mm, N_A : tensile yielding force in the anchorage bar, and H : height between the center of the foundation beam and the top floor beam, i.e., 1640 mm. The contribution of the anchorage bar at the base of the steel-braced frame to the lateral resistance was taken into account for Eqn. 4.2 since the anchorage bar yielded at the peak strength for both Specimens No.3 and No.2.

Q_{c1} and Q_{c4} in Eqn. 4.1 are the lateral shear resistance of R/C exterior columns (i.e., Columns 1 and 4 in **Fig. 1**) which was computed from ultimate bending moment.

Table 2 : Lateral strength of specimens

Specimen	Lateral strength in test, Q_{max}, kN	Predicted strength, Q_{cal}, kN	Q_{max} / Q_{cal}
No.3	251	267	0.94
No.2	270	254	1.06

While the lateral strength measured for Specimen No.3 subjected to out-of-plane loading was 0.94 times that predicted by Eqn. 4.1 as indicated in **Table 2**, the lateral strength measured for Specimen No.2 without out-of-plane loading was 1.06 times as large as that predicted. Due to out-of-plane loading, the lateral strength decreased to 89 percent (equal to 0.94/1.06) of that without out-of-plane loading, considering the difference in the concrete and steel strength. This degradation of the lateral strength resulted from severe compression damage of concrete at the bottom of boundary columns due to bi-axial bending. Therefore, the lateral resistant capacity, which was dominated by the column tension failure at the base of the steel-braced frame, was reduced by bi-directional horizontal loading.

4.3 Contribution of Elements to Lateral Resistance

Contribution of each element, that is, the steel-braced frame, R/C boundary columns and exterior columns, to lateral shear resistance of the specimens during the test is shown in **Fig. 8**. The lateral force resisted by the R/C central bay with the steel-braced frame, $Q_{Bf,exp}$, was computed as follows.

$$Q_{Bf,exp} = Q_{u,exp} - (Q_{c1,exp} + Q_{c4,exp}) \qquad (4.3)$$

where $Q_{u,exp}$: measured lateral shear resistance of the specimen corrected by P-Delta effect, and $Q_{c1,exp}$, $Q_{c4,exp}$: shear force resisted by the R/C exterior Columns 1 and 4, respectively, during the test which was computed from measured tensile strains in longitudinal bars at the top and bottom critical sections.

The lateral force, $Q_{Bf,exp}$, is divided into three components as follows, illustrated within **Fig. 8(a)** ;

$$Q_{Bf,exp} = Q_{br} + Q_2 + Q_3 \qquad (4.4)$$

where Q_{br} : lateral shear force shared by diagonal steel chords in the first-story braced frame, obtained in Chapter 4.1, and Q_2 , Q_3 : shear force in the R/C boundary Columns 2 and 3, respectively, with the vertical steel rim of the steel-braced frame.

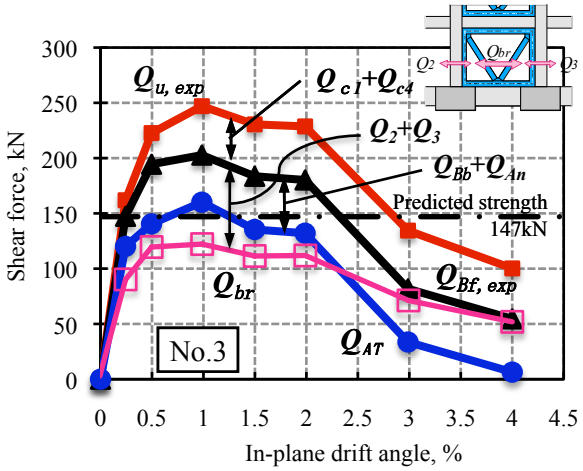

(a) Specimen No.3 under tri-lateral loading

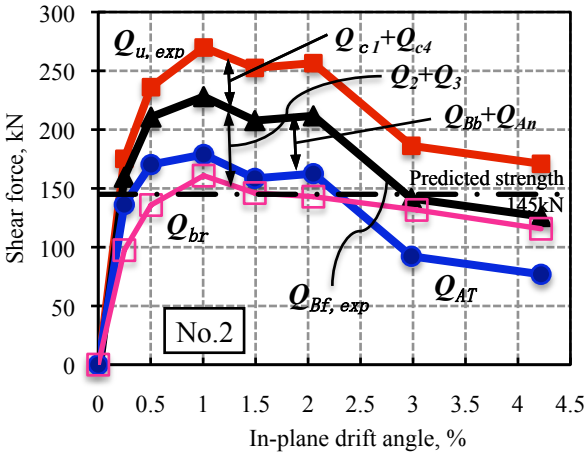

(b) Specimen No.2 without out-of-plane loading

Figure 8 : Contribution of elements to lateral resistance of frame

On the other hand, the lateral force, $Q_{Bf,exp}$, can be obtained alternatively by the same manner as Eqn. 4.2 using measured strains of longitudinal bars in boundary beams and columns and anchorage bars between the bottom of the steel-braced frame and the R/C foundation beam. Then the lateral force, Q_{AT}, derived from contribution due to both the compressive axial load applied to the steel-braced frame and the tensile force induced to the R/C boundary column, is computed as follows, and shown in **Fig.8**.

$$Q_{AT} = Q_{Bf,exp} - Q_{Bb} - Q_{An} \qquad (4.5)$$

Where Q_{Bb} : lateral resistant force due to the restraining moment of boundary beams connecting to the steel-braced frame, equal to $(\Sigma M_b + l_w \Sigma Q_b)/H$, and Q_{An} : lateral resistant force due to the pull-out resultant force of three anchorage bars at the bottom of the first story steel-braced frame, equal to $l_w' N_A / H$.

A horizontal dotted-and-broken line in **Fig. 8** represents the predicted lateral strength in the column tension failure according to the Japanese standard for evaluation of seismic capacity of existing R/C buildings (Ref. 2), which takes account of the contribution of the compressive axial load to the steel-braced frame and the tensile force induced to the R/C boundary column, corresponding to the aforementioned lateral resistance, Q_{AT}.

Peak strength of the lateral force, Q_{AT}, resisted by both the compressive axial load and the tensile force in the boundary column, obtained by the test, exceeded that predicted by the standard for both specimens. While the observed lateral force, Q_{AT}, for Specimen No.2 without out-of-plane loading was larger than the predicted peak strength till an in-plane drift angle of 2 %, the observed lateral force for Specimen No.3 subjected to out-of-plane loading became less than the predicted peak strength after the peak lateral shear capacity for the whole of the specimen. This indicates that while the prediction method by the standard (Ref. 2) for the lateral strength in the R/C bay with the multi-story steel-braced frame could appreciate the peak capacity without the contribution of both the confining effect due to boundary beams and the pull-out resistance of anchorage bars, the predicted lateral strength was not conservative after a drift angle of 1.5 % under tri-lateral loading.

4.4 Deformation Performance

Deformation capacity for a retrofitted R/C frame by a steel-braced frame, in which column tension failure occurs, can be estimated according to the standard (Ref. 2). Deformation capacity of a component is expressed in the standard by the ductility index denoted as F which is a function of the ductility factor as follows ;

$$F = \frac{\sqrt{2\,R_{mu}/R_y - 1}}{0.75(1 + 0.05\,R_{mu}/R_y)} \tag{4.6}$$

where R_{mu} : ultimate limit drift angle of R/C members and R_y : yielding drift angle assumed to be 0.67 % as specified by the standard.

Table 3 : Ultimate limit drift angle

Specimen	Predicted, %	Obtained by test, %		Ratio of obtained to predicted angle	
		Positive loading	Negative loading	Positive loading	Negative loading
No.3	1.72	2.20	2.50	1.28	1.45
No.2	1.68	3.07	3.09	1.83	1.84

The ductility index F obtained according to the standard (Ref. 1 in detail) was 2.41 for Specimen No.3 subjected to out-of-plane loading and 2.38 for Specimen No.2 without out-of-plane loading. These values correspond to an ultimate limit drift angle of 1.72 % and 1.68 % respectively, converted by Eqn. 4.6, as listed in **Table 3**.

On the other hand, the ultimate limit drift angle in the test was determined as shown in **Fig. 9**, which is defined as the drift angle when the lateral resistance descended to 80 percent of the peak strength for the envelope curve of the shear force - drift angle relationship. The measured ultimate drift angle for Specimen No.3 was 2.2 % in the positive loading direction and 2.5 % in the negative loading

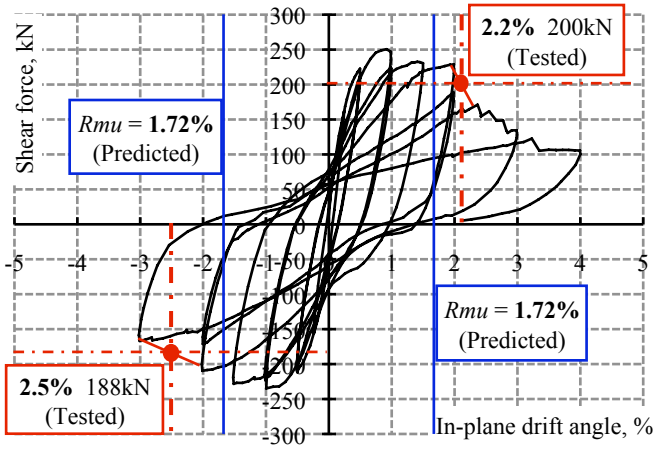

Figure 9 : Ultimate limit drift angle for Specimen No.3 under tri-lateral loading

direction, and the average angle was 1.37 times as large as that computed equal to 1.72 %. Therefore, computed ultimate limit deformation based on the ductility index *F* was regarded as conservative even under tri-lateral loading in comparison with the test result, although the lateral resistance decreased remarkably during the 2 % drift cyclic load reversals, and rupture of longitudinal bars in the boundary columns caused more degradation of the lateral resistance after a drift angle of 2 %. Deformation capacity under tri-lateral loading was inferior to that without out-of-plane loading as seen from **Table 3** since the ratio of measured to predicted ultimate limit deformation under tri-lateral loading was only 0.74 times that without out-of-plane loading.

5. CONCLUDING REMARKS

Lateral resistance and deformation capacity of a retrofitted R/C building by a multi-story steel-braced frame were studied by the tri-lateral loading test using a quarter-scale plane frame with two-stories and three-bays. The study described herein provides following conclusions under the limited condition that beams and columns in an existing R/C frame do not fail in shear but develop flexural yielding.

1) All longitudinal bars in a R/C boundary column adjacent to a steel-braced frame yielded in tension at a drift angle of 0.38 %. The lateral shear resistance reached peak capacity at a drift angle of approximately 1 %, forming plastic hinges at the end of all boundary beams. Hereafter lateral resistance reduced gradually by concrete compressive failure and fracture of longitudinal bars at the bottom of both boundary columns after a drift angle of 2 %.

2) The lateral shear strength, resulted from the column tension failure by the test under tri-lateral loading, was 6 percent less than that predicted by considering both resisting moment of boundary beams and tensile resistance of anchorage bars connecting the steel-braced frame to the R/C foundation beam. The ratio of measured lateral shear strength to predicted strength under tri-lateral loading was 10 percent less than that obtained by the previous test without out-of-plane loading. This shows that the lateral shear capacity was decreased by bi-directional horizontal loading. This was caused by severe compressive damage of concrete at the bottom of R/C boundary columns due to bi-axial bending.

3) Ultimate limit deformation in a retrofitted R/C frame failing in column tension at the bottom of a steel-braced frame was estimated conservatively by the Japanese standard (Ref. 2) even under tri-lateral earthquake excitations. However, deformation capacity under tri-lateral loading was inferior to that without out-of-plane loading due to bi-axial bending to R/C boundary columns adjacent to the steel-braced frame.

ACKNOWLEDGMENT

The study was sponsored by a Grant-in-aid for Scientific Research of Japan Society for the Promotion of Science (Researcher : K. Kitayama). Authors would like to express their gratitude to Dr. S. Kishida, associate professor in Shibaura Institute of Technology, and Mr. H. Hayashi, graduate student in Tokyo Metropolitan University, in conducting the experiment.

REFERENCES

1. KITAYAMA K. and KISHIDA S. (2004), Earthquake Resistant Performance of Reinforced Concrete Frame Strengthened by Multi-Story Steel Brace, *Proceedings of 13th World Conference on Earthquake Engineering*, CD-Rom, No.3266.
2. Japan Building Disaster Prevention Association, Standard for Evaluation of Seismic Capacity of Existing Reinforced Concrete Buildings, revised in 2001, (in Japanese).